FISEVIER

Contents lists available at SciVerse ScienceDirect

#### Thin Solid Films

journal homepage: www.elsevier.com/locate/tsf



## Correlation of electrolyte-derived inclusions to crystallization in the early stage of anodic oxide film growth on titanium

C. Jaeggi <sup>a,\*</sup>, M. Parlinska-Wojtan <sup>b</sup>, P. Kern <sup>c,1</sup>

- <sup>a</sup> Empa, Swiss Federal Laboratories for Materials Testing and Research, Advanced Materials Processing Laboratory, Feuerwerkerstrasse 39, CH-3602 Thun, Switzerland
- b Empa, Swiss Federal Laboratories for Materials Testing and Research, Center for Electron Microscopy, Ueberlandstrasse 129, CH-8600 Dübendorf, Switzerland
- <sup>c</sup> Empa, Swiss Federal Laboratories for Materials Testing and Research, Laboratory for Mechanics of Materials and Nanostructures, Feuerwerkerstrasse 39, CH-3602 Thun, Switzerland

#### ARTICLE INFO

# Article history: Received 19 January 2011 Received in revised form 11 August 2011 Accepted 25 August 2011 Available online 31 August 2011

Keywords:
Anodic oxide
Crystallization
Titania
Contamination
Nano-pores
Growth model

#### ABSTRACT

Pure titanium has been subjected to anodization in sulfuric and phosphoric acid. For a better understanding of the oxide growth and properties of the final film, with a particular interest focused on the solution anions in the early stage of crystallization, microstructural analyses (Raman, Transmission Electron Microscopy [TEM]) of the oxide films were correlated to chemical depth profiling by glow discharge optical emission spectroscopy (GDOES).

Raman spectroscopy shows that crystallization of the oxide films starts at potentials as low as 10–20 V. The onset of crystallization and the ongoing increase in crystallinity with increasing anodization potentials had already earlier been correlated to ac-impedance measurements [Jaeggi et al., Surf. Interface Anal. 38 (2006) 182]. TEM observations show a clear difference in the early phase of crystallization between oxides grown in 1 M sulfuric acid compared to 1 M phosphoric acid. Moreover, independent of electrolyte type, nano-sized pores from oxygen bubbles formation were revealed in the central part of the films. Until now, oxygen bubbles inside an anodically grown oxide have not been observed before without the presence of crystalline regions nearby. A growth model is proposed, in which the different starting locations of crystallization inside the films are correlated to the presence of the acid anions as residues in the film, as found by GDOES chemical depth-profiling.

© 2011 Elsevier B.V. All rights reserved.

#### 1. Introduction

Titanium as a material combining good mechanical strength and a low density is used in many technological areas such as aerospace, automotive industry, jewelry and medicine. Especially in the latter application its property of excellent corrosion resistance in most aqueous environments is very important, which is due to a thin passive film of a few nanometers forming spontaneously on the surface when oxygen is present [1]. Similar to all other valve metals, the native oxide thickness can be increased by anodic polarization and thus, thin (interference colored) coatings or thick porous coatings can be produced. Depending on the applied oxidation conditions (e.g. electrolyte type and concentration, potentials, etc.) the films can grow dense or porous, amorphous or crystalline, or as arrays of nanotubes [2–5]. For the application as bioactive material efforts are made to implement for example phosphorus and calcium into anodic titania [6].

Sul [7] has found that the bone response to oxidized implants was strongly influenced by the choice of anodization electrolytes.

Anodic oxidation of titanium is widely accepted to follow the highfield growth model [8–12]. The oxide growth takes place by ion migration and diffusion in the film, where the transport is explained by a thermally activated, field supported hopping. The film grows at both interfaces metal/oxide and oxide/electrolyte. The cationic transport is dominant in anodic TiO<sub>2</sub> [13], but the transport number (fraction of the film growth at the oxide/electrolyte interface compared to the entire oxide thickness) comes closer to 0.5 with increasing current density [14]. Crystallization in galvanostatically grown films has been found to start at potentials as low as 10-20 V [3,15]. Film crystallization and breakdown are related by Shibata et al. [4] to high internal compressive stress, caused by high electric field induced electrostriction. Habazaki et al. are the only authors in literature attributing a stabilization of amorphous oxide to the possible inclusion of electrolyte species together with substrate alloying elements in the oxide layer [15,16] on TiSi and TiAl systems anodized in pentaborate or phosphoric acid solution. There is still a lack of information on the influence of electrolytederived species on the crystallization of anodically formed titanium oxide layers.

Two electrolytes used regularly for anodization purposes are sulfuric acid and phosphoric acid. In previous works we have investigated the oxides produced in both of these electrolytes and compared

<sup>\*</sup> Corresponding author at: Empa, Swiss Federal Laboratories for Materials Testing and Research, Advanced Materials Processing Laboratory, Feuerwerkerstrasse 39, CH-3602 Thun, Switzerland. Tel.: +41 58 765 62 46; fax: +41 33 228 4490.

*E-mail addresses*: christian.jaeggi@empa.ch (C. Jaeggi), magdalena.parlinska@empa.ch (M. Parlinska-Wojtan), Philippe.Kern@neopac.ch (P. Kern).

<sup>&</sup>lt;sup>1</sup> Present address: Hoffmann Neopac AG, Burgdorfstrasse 22, CH-3672 Oberdiess-bach. Switzerland.

them with respect to film growth and chemical composition [17,18]. In the present investigation a microstructure-based growth model of the early stage of anodic growth is proposed. The aim is to correlate the crystallization onset with the stabilization of the amorphous titanium oxide phase by electrolyte derived inclusions.

#### 2. Experimental details

#### 2.1. Sample preparation and anodization

Commercially pure titanium disks (grade 2, purity  $\geq$  99.6%, Goodfellow UK) with a diameter of 15 mm and a thickness of approximately 1 mm were used. Their preparation to a surface roughness with  $R_a$  below 10 nm and the anodic oxidation setup are described in [17]. The electrolytes with a final concentration of 1 M were prepared from 95 to 97%  $H_2SO_4$  and 85%  $H_3PO_4$  (p.a. Merck), respectively. Anodic oxidation was performed potentiodynamically by applying a sweep rate of 5 V/s up to different end potentials, where it was stopped immediately (no hold time was applied). Samples were thoroughly rinsed with deionized water, then dried in a nitrogen jet.

#### 2.2. Raman spectroscopy

Raman spectra were measured in backscattering geometry on a Renishaw Ramascope 2000 using a HeNe-laser ( $\lambda$  = 633 nm). The power arriving on the substrate on the diffraction limited laser spot of about 2  $\mu$ m diameter was ~2 mW.

#### 2.3. Transmission Electron Microscopy (TEM)

Cross-sections from the oxidized titanium were cut by focused ion beam (FIB-Dual Beam FEI STRATA DB 235). The conventional TEM micrographs were taken with an EM-430 microscope operating at 300 keV, equipped with an LaB $_6$  cathode and a point resolution of 2.3 Å. The HRTEM images were performed on a Philips CM-300 FEG instrument operating at 300 keV with an information limit of 1.7 Å.

#### 2.4. Chemical depth profiling

GDOES (Jobin-Yvon 5000 RF) was used for estimation of film thickness and for chemical depth profiling. The measurements were made in rf mode with an rf-frequency of 13.56 MHz, argon gas pressure of 700 Pa, power of 60 W, with H and  $V_{\rm dc}$  corrections applied (for more details see [17] and [19]). For the quantification of Ti and O, calibration was performed by comparison to XPS analyses. For S contents, certified steels as well as a thoroughly characterized MoS2 reference samples were used for calibration. For P contents, also certified steels as well as thoroughly characterized chemical nickel reference samples were used. For quantitative depth calibration, reference anodic oxides were measured by FIB-prepared cross-sections as well as by spectral ellipsometry measurements.

#### 3. Results and discussion

#### 3.1. Anodization and oxide phase

The current response upon anodic oxidation was very well reproducible for both electrolytes: 1 M sulfuric acid (1 M HS) and 1 M phosphoric acid (1 M HP), respectively. Compared to 1 M HP, not only was the sparking potential in 1 M HS shifted to lower potentials ( $\sim$ 80 V for 1 M HS and  $\sim$ 150 V for 1 M HP, the latter is not shown here, see also [18]), but also the anodization current was clearly higher, as shown in Fig. 1.

Considering the fact that the growth rate of the produced oxides in 1 M HP is only marginally smaller than in 1 M HS ( $\sim$ 2 nm/V, see [18]), with the 1 M HP oxides being thinner by up to  $\sim$ 10 nm at a given

anodization potential up to 80 V, this indicates a higher current efficiency of the HP electrolyte at potentials higher than ~10 V. This means that less oxygen is produced as a side reaction, which may be related to a different microstructure of the formed oxide (see also section 3.5).

For both electrolytes partial crystallization appears to start at potentials as low as 10 V, as evidenced by Raman measurements (most prominent peak of the anatase phase at  $\sim 144 \text{ cm}^{-1}$ ). However, the degree of crystallinity is generally more pronounced for oxides grown in 1 M HS as compared to 1 M HP, as shown by Raman spectroscopy in Fig. 2. A 100 V 1 M HP oxide shows about the same Raman signal as a 50 V 1 M HS oxide. Additionally, with increased anodization potential, the 1 M HS films show a clear anatase phase pattern that gradually transforms into rutile beyond the sparking potential. Oxides grown in 1 M HP, however, never show a clear one-phase anatase signal, but rather a mixed phase of anatase and a diffuse signal of most possibly rutile. This is in accordance with the generally lower anodization currents leading to less heating, which could induce the transformation. The general trend of the ongoing crystallization with increasing anodization potentials has been linked to ac-impedance measurements already in earlier works [17,18] by following the evolution of film capacitance and resistance values.

#### 3.2. Microstructure

The early crystallization at low potentials, as found by Raman, was verified for both electrolyte types by TEM investigations. The TEM micrographs in Fig. 3 were taken from focused ion beam (FIB)-cut cross sections of oxide layers grown to 20 V in 1 M HP (Fig. 3a) and 1 M HS (Fig. 3b), respectively. Comparing the lower magnification overview images shown as inserts in the respective figures, both oxides show a multilayer structure with some internal porosity: a dense interfacial part, next to the metal-oxide interface, a porous central part and again a dense outer layer. Comparing the coatings formed in the two electrolytes at higher resolution, crystallization was found to start in different regions of the oxide. The 20 V oxide grown in 1 M HP shows some nanocrystalline regions exclusively in the interfacial dense part of the layer directly adjacent to the interface oxidemetal, with the central porous part and the outer dense part still being amorphous (Fig. 3a). On the other hand, the 20 V 1 M HS oxide shows nanocrystallite formation almost exclusively in the outermost oxide layer as well as around the porous central part (Fig. 3b). Also, supporting the trend observed by Raman, the HP oxide features less crystallinity at this given anodization potential compared to the corresponding HS oxide. These trends are not only seen in high resolution TEM images, but could also be followed on

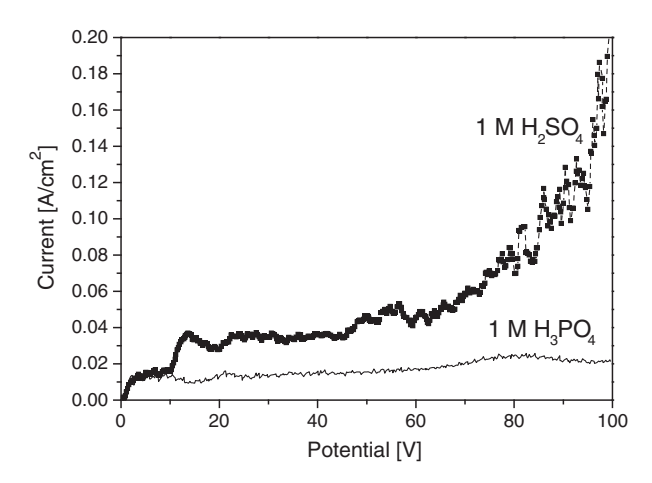


Fig. 1. Anodic oxidation curve of Ti in 1 M  $\rm H_2SO_4$  (dotted line) and 1 M  $\rm H_3PO_4$ . Sweep rate was always 5 V/s.

#### Download English Version:

### https://daneshyari.com/en/article/1667313

Download Persian Version:

https://daneshyari.com/article/1667313

<u>Daneshyari.com</u>